Available online at www.sciencedirect.com
SCIENCE DIRECT
Journal of Solid State Chemistry 179 (2006) 1407–1414
JOURNAL OF SOLID STATE CHEMISTRY
www.elsevier.com/locate/jssc

Layer-by-layer assembly of multilayer films of polyoxometalates and tris(phenanthrolinedione) complexes of transition metals

Shuiying Gao[a,b], Xing Li[a], Chunpeng Yang[a], Taohai Li[a,b], Rong Cao[a,*]

[a]*State Key Laboratory of Structural Chemistry, Fujian Institute of Research on the Structure of Matter, The Chinese Academy of Sciences, Fuzhou 350002, China*

[b]*Graduate School of The Chinese Academy of Sciences, Beijing 100039, China*

Received 8 December 2005; received in revised form 23 January 2006; accepted 29 January 2006
Available online 9 March 2006

Abstract

A series of organic–inorganic composite films were prepared by the layer-by-layer self-assembly method containing the phendione complexes of transition metals $[M(\text{phendione})_3]^{2+}$ ($M = Fe^{2+}$, Co^{2+}, phendione = 1,10-phenanthroline-5,6-dione) and the polyoxometalates (POMs). UV–vis spectroscopy was used to follow the fabrication process of $(BW_{12}/[M(\text{phendione})_3]^{2+})_n$ ($BW_{12} = BW_{12}O_{40}^{5-}$, $M = Fe^{2+}$, Co^{2+}) and $(Co_4(PW_9)_2/[M(\text{phendione})_3]^{2+})_n$ ($Co_4(PW_9)_2 = Co_4(H_2O)_2(PW_9O_{34})_2^{10-}$, $M = Fe^{2+}$, Co^{2+}) multilayer films. Electrochemical studies on the films illustrate that the POM species exhibit well-defined redox peaks and the phendione species show pH-dependent electrochemical behavior. The photoluminescent properties were investigated to show the $(BW_{12}/[Fe(\text{phendione})_3]^{2+})_n$ film with low-energy red photoluminescence at 672 nm.

Keywords: Polyoxometalates; Layer-by-layer self-assembly; 1,10-Phenanthroline-5,6-dione; Photoluminescence

1. Introduction

The fabrication of functional ultrathin films has received considerable interest in materials chemistry due to their nanostructural and nanosized effect [1–4]. The layer-by-layer self-assembly method proposed by Decher is based on electrostatic interactions between cationic and anionic polymers [5]. This method is a simple but powerful, versatile, and economical technique, independent of substrate size and topology. Therefore, the method has been widely employed for the fabrication of ultrathin films of charged materials such as charged polymers [6,7], organic dyes [8–10], bimoleculars [11,12], nanoparticles [13,14], etc. Polyoxometalates (POMs) as typical inorganic metal oxide clusters [15], are very versatile inorganic building blocks for the construction of functional thin films. POMs are used as the anionic moiety to attract and bond multiply charged cations in self-assembled multilayers [3,16,17]. On the other hand, functional multilayer films containing POMs have potential application in electrocatalytic [18], electrochromic [19] and photoluminescent materials [20]. For example, POMs containing rare earth metal have been used to construct photoluminescent films with cationic polyelectrolytes [20]. However, the POMs functional multilayers reported to date are mainly composed of negatively charged POMs and positively charged polyelectrolytes, the transition metal complexes as the charge-balancing species in film fabrication are rarely reported. Transition metal complexes as the charge-balancing species are especially fascinating because of their unique properties with well-defined surface functionality compared to conventional polyelectrolytes [16,19,21–23]. Only a few examples such as multilayer films of $Os(bpy)_3^{2+}$–$P_2Mo_{18}O_{62}^{6-}$ and $Ru(bpy)_3^{2+}$–$P_2Mo_{18}O_{62}^{6-}$ were reported [21,22], and the studies mainly focused on the properties of transition metal ions rather than ligands. In order to explore the potential application of transition metal complexes in the nanostructural materials, it is important to design, fabricate, and study functional films containing functional ligands.

1,10-Phenanthroline-5,6-dione (phendione) is particularly attractive because it carries an *o*-quinone moiety with

*Corresponding author. Fax: +86 59183796710.
E-mail address: rcao@ms.fjirsm.ac.cn (R. Cao).

0022-4596/$ - see front matter © 2006 Elsevier Inc. All rights reserved.
doi:10.1016/j.jssc.2006.01.069

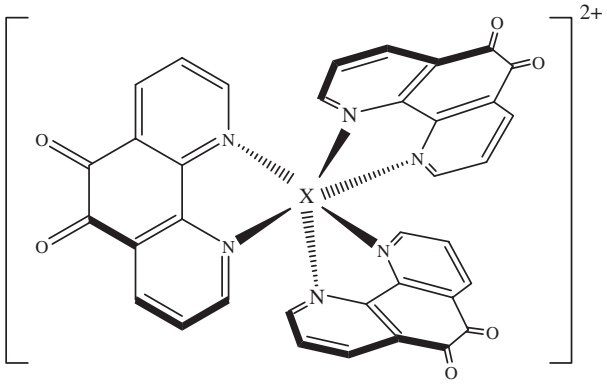

1 X = Fe^{2+}
2 X = Co^{2+}

Scheme 1. The structures of $[Fe(phendione)_3]^{2+}$ (**1**) and $[Co(phendione)_3]^{2+}$ (**2**) complexes.

pH-dependent electroactivity [24]. The ligand forms stable complexes with transition metal ions and shows the electrocatalytic activity toward the oxidation of NADH (dihydronicotinamide adenine dinucleotide) [25]. Moreover, metal complexes of the ligand also change the potentials through pH changes. Therefore, $[Fe(phendione)_3]^{2+}$ and $[Co(phendione)_3]^{2+}$ complexes (Scheme 1), which make them promising candidates, are used as large and multiply charged cations to construct the multilayers with anionic POMs in our study.

In this report, we present the fabrication of ultrathin organic–inorganic composite films of phendione complexes of transition metals and POMs by the layer-by-layer self-assembly method. The functional films are characterized by UV–vis spectroscopy. The electrochemical behavior of the phendione complexes of the films was investigated in different pH values by cyclic voltammogram. The photoluminescence properties of the films have also been investigated by fluorescence spectroscopy.

2. Experimental section

2.1. Materials

Poly(ethylenimine) (PEI, 50 wt% aqueous solution) was purchased from Aldrich Chemical Co. $K_5BW_{12}O_{40}$ (BW_{12}) and $K_{10}Co_4(H_2O)_2(PW_9O_{34})_2$ ($Co_4(PW_9)_2$) were prepared by published methods [26,27]. Phendione and its complexes $[Fe(phendione)_3](PF_6)_2$ and $[Co(phendione)_3](PF_6)_2$ were synthesized according to Refs. [24,25,28]. All other reagents were of analytical grade and used as received. Buffer solutions were prepared from 0.2 M NaAc + 0.3 M HAc.

2.2. Preparation of the multilayers

The quartz slides were cleaned with a "piranha solution" at 80 °C for 40 min, and thoroughly rinsed with distilled water. Further purification was carried out by immersion in a $H_2O/H_2O_2/NH_3OH$ (5:1:1) (V/V/V) bath for 30 min at 70 °C.

2.2.1. Preparation of PEI–$(Co_4(PW_9)_2/[Fe(phendione)_3]^{2+})_n$ multilayer films

The clean quartz slides were immersed in aqueous solution of PEI (10 mg ml^{-1}) for 20 min, washing with water and drying with nitrogen stream. The pre-coated quartz slides were then alternately immersed in $Co_4(PW_9)_2$ (5 mM) aqueous solution and $[Fe(phendione)_3](PF_6)_2$ (12 mM) acetonitrile solution for 20 min. After each immersion, the substrates were rinsed with water and dried with nitrogen gas. Multilayer films on solid substrates could be formed by repeating the above steps in a cyclic fashion.

2.2.2. Preparation of PEI–$(Co_4(PW_9)_2/[Co(phendione)_3]^{2+})_n$ multilayer films

The clean quartz slides were immersed in aqueous solution of PEI (10 mg ml^{-1}) for 20 min, washing with water and drying with nitrogen stream. The pre-coated quartz slides were then alternately dipped into aqueous solution of $Co_4(PW_9)_2$ (5 mM) and $[Co(phendione)_3](PF_6)_2$ (8 mM) acetonitrile solution for 20 min.After each immersion, the substrates were washed with water and dried with nitrogen gas.

2.2.3. Preparation of PEI–$(BW_{12}/[M(phendione)_3]^{2+})_n$ ($M = Fe^{2+}$, Co^{2+}) multilayer films

The clean quartz slides were immersed in aqueous solution of PEI (10 mg ml^{-1}) for 20 min, washed with water and dried with nitrogen stream. The pre-coated quartz slides were then alternately immersed in aqueous solution of 4×10^{-2} M BW_{12} and $[M(phendione)_3](PF_6)_2$ (12 mM $[Fe(phendione)_3](PF_6)_2$ or 8 mM $[Co(phendione)_3](PF_6)_2$ for 20 min. After each immersion, the substrates were washed with water and dried with nitrogen gas.

2.3. Characterization of the films

UV–vis absorption spectra were recorded on a quartz slide using a Lambda35 spectrophotometer (Perkin-Elmer, USA). AFM images were taken on a quartz slide using a Nanoscope IIIa (Digital Instruments Inc., Veeco, USA) operating in the tapping mode with silicon tips.

Electrochemical experiments were carried out on an Epsilon Analyzer (BAS Inc., USA) in a three-electrode cell: glassy carbon electrode (GCE, diameter 3 mm) as working electrode, platinum wire as counter electrode, and Ag/AgCl/KCl (3 M) as reference electrode. Prior to modification, GCE was successively polished with 1.0 and 0.3 μm α-Al_2O_3 and ultrasonically washed with acetone and water between each experiment. Then, the GCE was modified with the multilayers. The procedure of electrode modification was as follows: The clean electrode was coated with PEI to introduce a positive charge onto its

surface. Then the PEI-coated electrode was alternately dipped into POMs (5 mM $Co_4(PW_9)_2$ or 4×10^{-2} M BW_{12}) solution and $[M(phendione)_3](PF_6)_2$ (12 mM [Fe(phendione)$_3$] $(PF_6)_2$ or 8 mM [Co(phendione)$_3$] $(PF_6)_2$) solution for 20 min each, followed by rinsing and drying. The solutions were deaerated with prepurified nitrogen for at least 15 min. Formal potentials E_p of the redox couples were estimated and reported as the average values of the anodic (E_{pa}) and cathodic (E_{pc}) peak potentials.

Photoluminescence spectra were obtained at room temperature with a FLS920 fluorescence spectrophotometer (EDINbergh Instruments, British).

3. Results and discussion

UV–vis spectroscopy is used to monitor the layer-by-layer self-assembly process of organic–inorganic composite films. Fig. 1 shows the UV–vis absorption spectra of the multilayers assembled on quartz substrates. For PEI–$(Co_4(PW_9)_2/[Fe(phendione)_3]^{2+})_n$ multilayer films (Fig. 1a), the absorption peak at 250 nm is ascribed to $Co_4(PW_9)_2$ polyanion, whereas the absorption peak at 312 nm is from the phendione ligand-centered π–π^* transitions. The broad absorption band around 510 nm in the visible region is due to metal-to-ligand charge transfer (MLCT) transition in the $[Fe(phendione)_3]^{2+}$ film. The UV–vis spectrum of an aqueous $Co_4(PW_9)_2$ solution indicates one characteristic absorption at 250 nm. Thus, the characteristic absorption at 250 nm can be employed to monitor the film growth. The inset in Fig. 1a presents the plots of the absorbance values for these multilayer films at 250 and 312 nm as a function of the number of deposition cycles, indicating the regular growth of the absorbance. For PEI–$(Co_4(PW_9)_2/[Co(phendione)_3]^{2+})_n$ films (Fig. 1b), the absorption peak at 250 nm is from the $Co_4(PW_9)_2$, whereas the absorption peak at 312 nm is due to the phendione ligand-centered π–π^* transitions. However, no absorption peak is observed in the visible region, indicating there is no charge transition in MLCT transition in $[Co(phendione)_3]^{2+}$ complex. The result is consistent with the reported literature [24]. For PEI–$(BW_{12}/[Fe(phendione)_3]^{2+})_n$ and PEI–$(BW_{12}/[Co(phendione)_3]^{2+})_n$ multilayers (Fig. 1c and d), it was found that the absorption peak at 259 nm was from the BW_{12} polyoxoanion and the absorption peak at 312 nm was from phendione ligand. Compared with $(BW_{12}/[Co(phendione)_3]^{2+})_n$ multilayers, $(BW_{12}/[Fe(phendione)_3]^{2+})_n$ multilayers have the broad

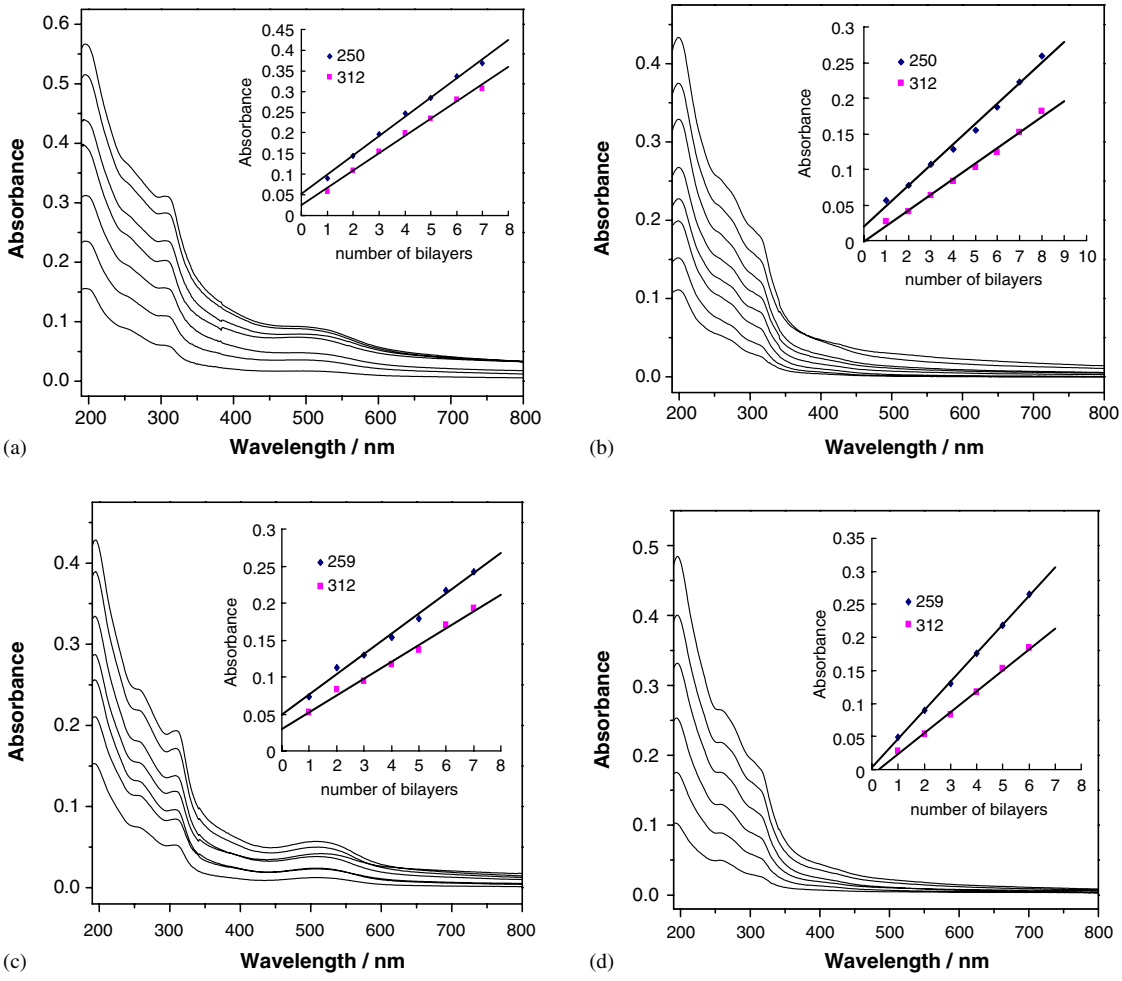

Fig. 1. UV–vis absorption spectra of the multilayer films: (a) PEI–$(Co_4(PW_9)_2/[Fe(phendione)_3]^{2+})_n$; (b) PEI–$(Co_4(PW_9)_2/[Co(phendione)_3]^{2+})_n$; (c) PEI–$(BW_{12}/[Fe(phendione)_3]^{2+})_n$; (d) PEI–$(BW_{12}/[Co(phendione)_3]^{2+})_n$.

absorption band around 510 nm in the visible region, due to MLCT transition of $[Fe(phendione)_3]^{2+}$.

The absorption spectra exhibit the characteristic peaks of the POMs and the metal complexes, suggesting phendione metal complexes can be used as large, multiply charged cations with anonic POMs to self-assembly multilayers. Moreover, for the films containing $[Fe(phendione)_3]^{2+}$, the absorption spectra indicate the broad band in the visible region, whereas the films with $[Co(phendione)_3]^{2+}$ show no absorption band in the visible region. All the multilayer films were stable, because their UV–vis spectra still remained unchanged after they were placed in air for several months.

In order to obtain the surface morphology information of the deposited films, atomic force microscopy (AFM) images of the multilayer films were obtained (shown in Fig. 2). As seen in Fig. 2, the composite film is relatively uniform and smooth. Their surfaces exhibit a granular texture. This reflects that the polyoxoanions aggregated to a certain level. Furthermore, the root-mean-square (RMS) of $(BW_{12}/[Fe(phendione)_3]^{2+})_4$–$BW_{12}$ and $(Co_4(PW_9)_2/[Fe(phendione)_3]^{2+})_4$–$Co_4(PW_9)_2$ surfaces was determined to be 2.510 and 4.899 nm calculated over an area of $1.0 \times 1.0\,\mu m^2$, respectively (Fig. 2a and b), while the RMS of $(BW_{12}/[Co(phendione)_3]^{2+})_4$–$BW_{12}$ and $(Co_4(PW_9)_2/[Co(phendione)_3]^{2+})_4$–$Co_4(PW_9)_2$ surfaces was determined to be 0.866 and 2.033 nm calculated over an area of $1.0 \times 1.0\,\mu m^2$, respectively (Fig. 2c and d). It was found that the RMS of the multilayer films with BW_{12} polyoxoanions is smaller than the films with $Co_4(PW_9)_2$ polyoxoanions. This indicates large size of $Co_4(PW_9)_2$ results in high RMS.

Cyclic voltammetry (CV) was used to investigate the electrochemical behavior of the multilayers. We investigated two bilayers, because it is difficult for a substrate to access the inner layers in the multilayer films with more layer numbers. Fig. 3 indicates the electrochemical behaviors of the multilayers at different scan rates. For PEI–$(Co_4(PW_9)_2/[Fe(phendione)_3]^{2+})_2$ multilayers, three redox peaks occur at potentials (E_p) of −0.744, −0.629 and −0.469 V in the negative potential due to the redox of $Co_4(PW_9)_2$ polyoxoanions, whereas the redox peak at +0.300 V (E_p) in the positive potential is due to phendione ligand (Fig. 3a). CV of the aqueous $Co_4(PW_9)_2$ polyanion was also investigated in buffer acetate solution (pH 4.4). It was found that the Co^{II} species do not show electroactivity in the positive potential region in buffer acetate solution. It was reported that the Co^{II} species do not exhibit electroactivity in the electrochemical studies of the aqueous $[Co_4(H_2O)_2(P_2W_{15}O_{56})_2]^{16-}$ polyoxoanion by Ruhlmann et al. [29], since the structure of $[Co_4(H_2O)_2(P_2W_{15}O_{56})_2]^{16-}$ polyoxoanion is similar to that of tetranuclear sandwich complexes $Co_4(PW_9)_2$. Therefore, the redox peak at +0.300 V (E_p) is ascribed to the phendione ligand. For PEI–$(Co_4(PW_9)_2/[Co(phendione)_3]^{2+})_2$, the electrochemical behaviors of the multilayers are similar to $(Co_4(PW_9)_2/$

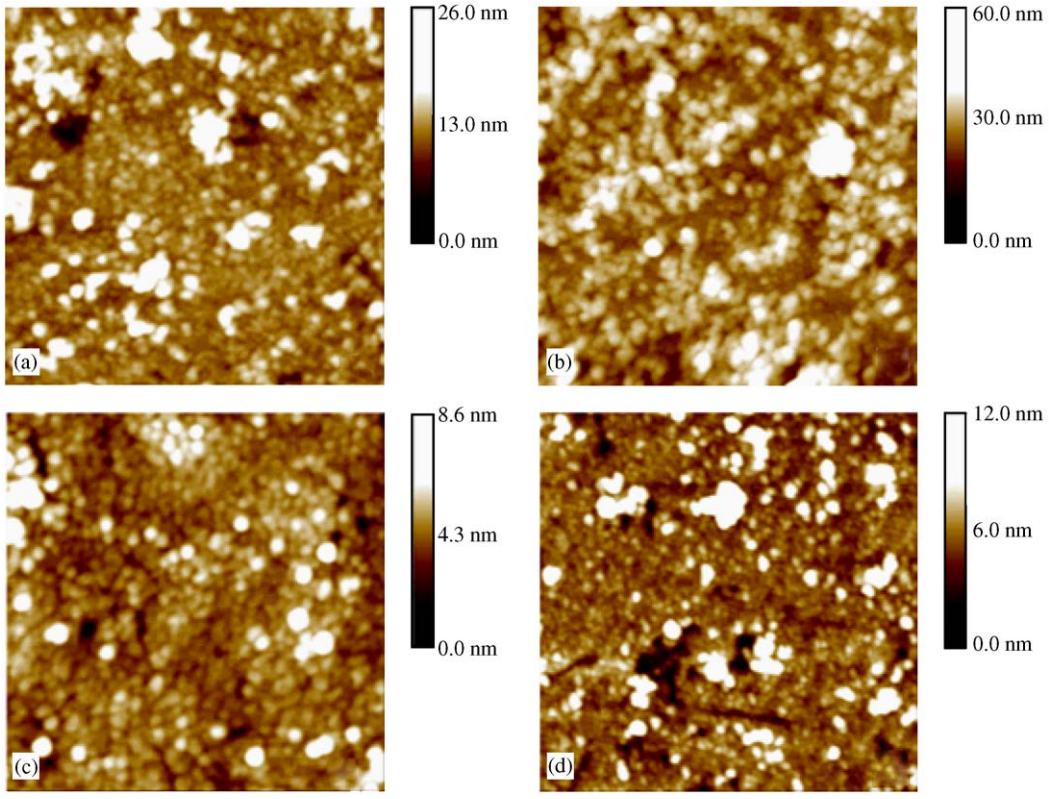

Fig. 2. AFM images of the multilayers on quartz slides. (a) PEI–$(BW_{12}/[Fe(phendione)_3]^{2+})_4$–$BW_{12}$; (b) PEI–$(Co_4(PW_9)_2/[Fe(phendione)_3]^{2+})_4$–$Co_4(PW_9)_2$; (c) PEI–$(BW_{12}/[Co(phendione)_3]^{2+})_4$–$BW_{12}$; (d) PEI–$(Co_4(PW_9)_2/[Co(phendione)_3]^{2+})_4$–$Co_4(PW_9)_2$ ($1.0 \times 1.0\,\mu m^2$).

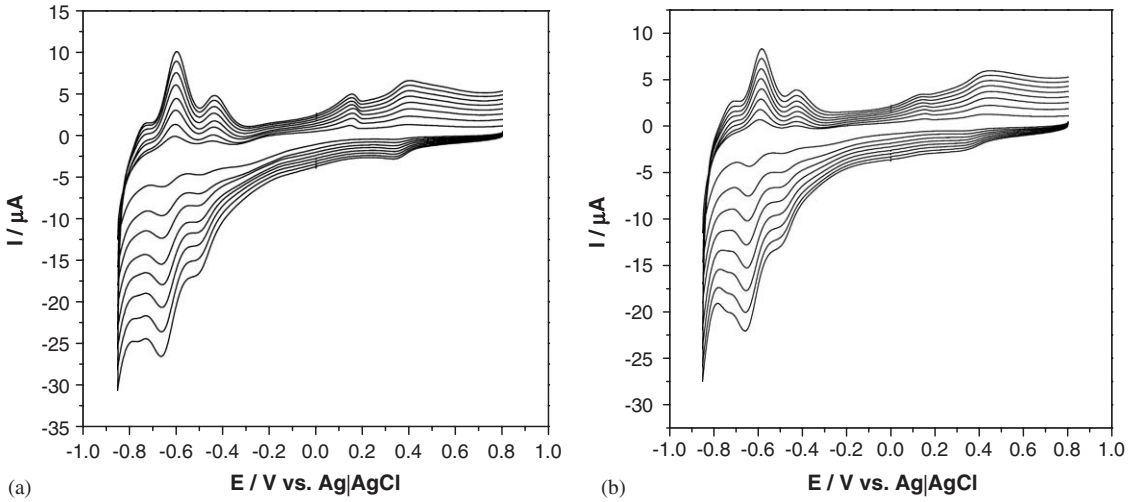

Fig. 3. Cyclic voltammograms of the multilayers in buffer solution (pH 4.4) at different scan rates. (a) PEI–$(Co_4(PW_9)_2/[Fe(phendione)_3]^{2+})_2$; (b) PEI–$(Co_4(PW_9)_2/[Co(phendione)_3]^{2+})_2$. Scan rate: 50, 100, 150, 200, 250, 300, 350, 400 mV s^{-1}.

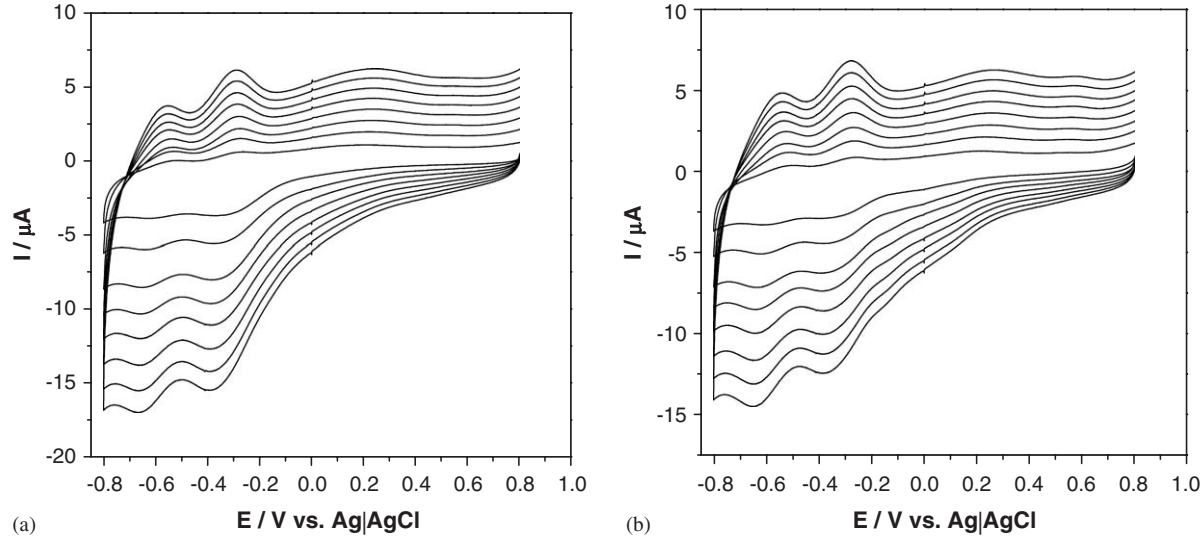

Fig. 4. Cyclic voltammograms of the multilayers in NaCl solution at different scan rates. (a) PEI–$(BW_{12}/[Fe(phendione)_3]^{2+})_2$; (b) PEI–$(BW_{12}/[Co(phendione)_3]^{2+})_2$. Scan rate: 50, 100, 150, 200, 250, 300, 350, 400 mV s^{-1}.

$[Fe(phendione)_3]^{2+})_2$ multilayers (Fig. 3b). Likewise, the redox peak at +0.379 V (E_p) in the positive potential is due to phendione ligand. The redox peak of the phendione in the positive potential is assigned to the two-electron/two-proton reduction of the quinone moiety to the corresponding hydro-quinone in acid media. The redox process of metal ions in $[Fe(phendione)_3]^{2+}$ and $[Co(phendione)_3]^{2+}$ complexes was not observed for the multilayer films, probably due to the fact that $[Fe(phendione)_3]^{2+}$ and $[Co(phendione)_3]^{2+}$ are relatively stable compared to the oxidized state. When the polyoxoanion $Co_4(PW_9)_2$ is replaced by BW_{12} polyoxoanion, the phendione ligand shows one irreversible broad peak around 0.100 V (E_{pa}) in neutral media in the positive potential. Two redox peaks in the negative potential are ascribed to the BW_{12} polyoxoanions (Fig. 4a and b), which occur at potentials (E_p) of −0.603 and −0.377 V, respectively. Moreover, the electrochemical behaviors of PEI–$(BW_{12}/[Fe(phendione)_3]^{2+})_2$ and PEI–$(BW_{12}/[Co(phendione)_3]^{2+})_2$ multilayer films were also studied in buffer acetate solution (pH 4.4) (as shown in Fig. 5). In the negative potential region, the redox peaks are ascribed to the BW_{12} polyoxoanions, whereas one irreversible broad peak is due to the phendione ligand in the positive potential region. The peak potentials of the phendione ligand in PEI–$(BW_{12}/[Fe(phendione)_3]^{2+})_2$ and PEI–$(BW_{12}/[Co(phendione)_3]^{2+})_2$ multilayer films occur at +0.306 and +0.300 V, respectively. Apparently, when the pH value is decreased to 4.4, the redox peak of the phendione become positively shifted and the reodx peaks of the BW_{12} polyoxoanion become irreversible. Therefore, the

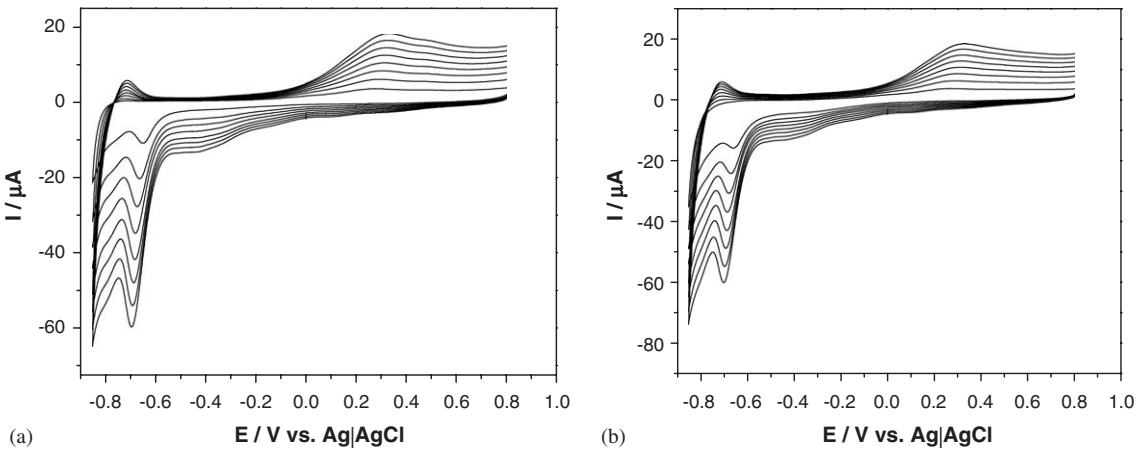

Fig. 5. Cyclic voltammograms of the multilayers in buffer solution (pH 4.4) solution at different scan rates. (a) PEI–$(BW_{12}/[Fe(phendione)_3]^{2+})_2$; (b) PEI–$(BW_{12}/[Co(phendione)_3]^{2+})_2$. Scan rate: 50, 100, 150, 200, 250, 300, 350, 400 mV s^{-1}.

electrochemical behaviors of the BW_{12} polyoxoanion and phendione in the multilayer films are pH dependent. Cyclic voltammograms of $[Fe(phendione)_3]^{2+}$ and $[Co(phendione)_3]^{2+}$ in the multilayers indicated that the phendione ligands were electroactive in buffer acetate solution at the potential of around +0.300 V. The small variations in potentials were ascribed to transition metal ions [25] and the polyoxoanions. It was found that the peak potentials were independent of scan rate and that the peak currents were directly proportional to scan rates of up to 0.4 V s^{-1}, indicating surface-controlled processes.

From the above result analyses, the electrochemical behaviors of POMs and transition metal complexes remain in the multilayer films and the behaviors is pH dependent. Therefore, the multilayer films have potential application in electrochemical sensors.

The electrocatalytic reduction of two substrates, NO_2^- and H_2O_2, by the multilayer films was investigated. Nitrite is a common pollutant from both agricultural and industrial sources [16]. The direct reduction of nitrite at bare carbon electrodes require a high overpotential. A large variety of POMs was reported for the electrocatalytic reduction of nitrite [3,18,30–32]. Fig. 6 shows the electrocatalytic reduction toward NO_2^-. Fig. 6a exhibits the cyclic voltammogram with PEI–$(Co_4(PW_9)_2/[Fe(phendione)_3]^{2+})_2$ in the absence of NO_2^-. The redox peaks of $Co_4(PW_9)_2$ polyoxoanion still remain. However, upon the additions of nitrite, the cathodic peak current of $Co_4(PW_9)_2$ increased greatly and the corresponding anodic peak current disappears completely. This clearly indicates that the nitrite ion is electrocatalytically reduced by the $Co_4(PW_9)_2$ polyoxoanion in PEI–$(Co_4(PW_9)_2/[Fe(phendione)_3]^{2+})_2$ film. Under our experimental condition, NO_2^- is the major species due to disproportionation reaction HNO_2 at pH value 4.4 [16]. The $Co_4(PW_9)_2$ polyoxoanion reduces the NO_2^- to NO, which substitutes water molecules in the labile site coordinated with transition metal Co forming transition metal nitrosyl

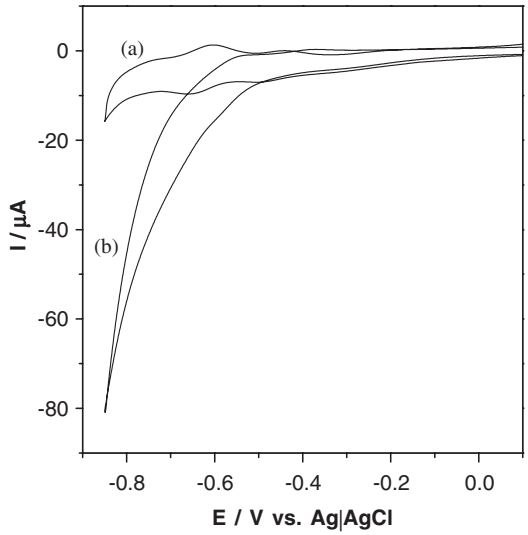

Fig. 6. Cyclic voltammograms at GCE modified with PEI–$(Co_4(PW_9)_2/[Fe(phendione)_3]^{2+})_2$ multilayer film in pH 4.4 buffer solutions before (a) and after (b) the addition of 2.5 mM NO_2^-. Scan rate: 100 mV s^{-1}.

complexes [33]. Moreover, the PEI–$(Co_4(PW_9)_2/[Fe(phendione)_3]^{2+})_2$ film exhibits the electrocatalytic reduction of H_2O_2 (Fig. 7). The electrochemical reduction of H_2O_2 into water is of great interest due to its application in biosensors and fuel cells [34,35]. By increasing the concentration of H_2O_2, the cathodic peak current increased, while its anodic peak current decreased. This shows a typical electrocatalytic reduction process. H_2O_2 is electrocatalytically reduced by the $Co_4(PW_9)_2$ polyoxoanion in PEI–$(Co_4(PW_9)_2/[Fe(phendione)_3]^{2+})_2$ film. The inset indicates the electrocatalytic current increases linearly with the concentration of H_2O_2 (Fig. 7). The possible mechanism of the catalytic process is ascribed to the intermediate formation of a peroxo complex between $Co_4(PW_9)_2$ polyoxoanion and hydrogen peroxide, which leads to a weakening of the oxygen–oxygen bond [34]. Therefore, the multilayers

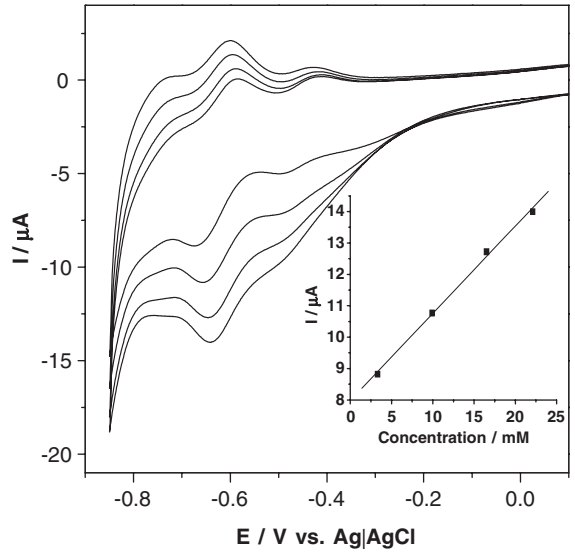

Fig. 7. Cyclic voltammograms at GCE modified with PEI–$(Co_4(PW_9)_2/[Fe(phendione)_3]^{2+})_2$ multilayer film in pH 4.4 buffer solutions containing H_2O_2 in various concentrations: 3.3, 9.9, 16.5, 22.1 mM. Scan rate: 100 mV s^{-1}.

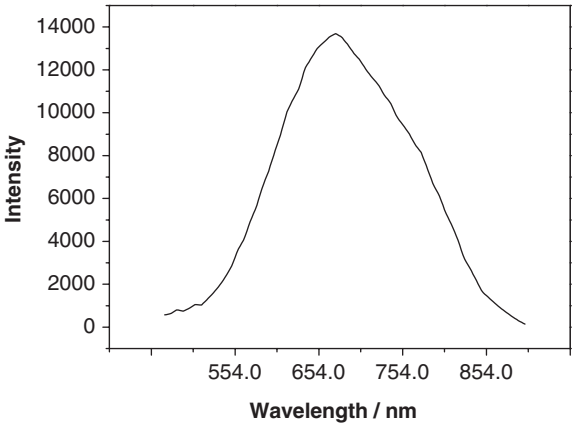

Fig. 8. The emission spectroscopy of PEI–$(BW_{12}/[Fe(phendione)_3]^{2+})_7$ multilayer film at room temperature ($\lambda_{ex} = 270$ nm).

exhibit the good electrocatalytic reduction of NO_2^- and H_2O_2.

The photoluminescence of the multilayer films was also investigated. It was found that $(BW_{12}/[Fe(phendione)_3]^{2+})_7$ films exhibits an emission maximum at 672 nm ($\lambda_{ex} = 270$ nm) (Fig. 8), whereas the multilayers containing $[Co(phendione)_3]^{2+}$ do not show detectable photoluminescence. It was investigated that the photoluminescent emission of the solid phendione exhibited blue emission at 490 nm. Hence the emission with $(BW_{12}/[Fe(phendione)_3]^{2+})_7$ is red-shifted compared to the phendione. It is ascribed to MLCT absorption at 510 nm in $[Fe(phendione)_3]^{2+}$ films. This is possibly because the strong electrostatic interaction between BW_{12} polyoxoanion and $[Fe(phendione)_3]^{2+}$ results in the change of the crystal field of $[Fe(phendione)_3]^{2+}$ [23]. The change is that the energy of the *d–d* states is above the MLCT state. In addition, BW_{12} component of the film increases spin–orbit coupling, which enhances the allowedness of the normally forbidden transition to the ground state. Thus, the complex $[Fe(phendione)_3]^{2+}$ of the film is transited from the singlet MLCT state to the triplet MLCT state through intersystem crossing, which results in the longer wavelength emission with $(BW_{12}/[Fe(phendione)_3]^{2+})_7$. The multilayers containing $[Co(phendione)_3]^{2+}$ do not show photoluminescence due to the absence of MLCT transition. Thus, it is understandable that no photoluminescent properties were observed for $[Co(phendione)_3]^{2+}$ films. Interestingly, the multilayer film of $(Co_4(PW_9)_2/[Fe(phendione)_3]^{2+})_8$ also has no emission at room temperature, indicating the photoluminescent properties of the films are influenced by the component of the films.

4. Conclusion

In this paper, we have prepared ultrathin organic–inorganic composite films that incorporate the phendione complexes of transition metals and the POMs. CV demonstrates $[Fe(phendione)_3]^{2+}$ and $[Co(phendione)_3]^{2+}$ of the films exhibit different electrochemical behaviors in various pH values. The POMs of the multilayer film exhibit electrocatalytic reduction of nitrite and hydrogen peroxide. Therefore, the multilayer films have potential applications as electrochemical sensors. The photoluminescent properties of the multilayer films indicate that the film with $(BW_{12}/[Fe(phendione)_3]^{2+})$ emits low-energy red photoluminesce at room temperature.

Acknowledgments

This work was financially supported by the financial support from NNSF of China (90206040, 20325106, 50472021), NSF of Fujian Province (E0520003), and the "One Hundred Talent" project from CAS.

References

[1] D.L. Feldheim, K.C. Grabar, M.J. Natan, T.E. Mallouk, J. Am. Chem. Soc. 118 (1996) 7640.
[2] H. Krass, E.A. Plummer, J.M. Haider, P.R. Barker, N.W. Alcock, Z. Pikramenou, M.J. Hannon, D.G. Kurth, Angew. Chem. Int. Ed. 40 (2001) 3862.
[3] L. Bi, H. Wang, Y. Shen, E. Wang, S. Dong, Electrochem. Commun. 5 (2003) 913.
[4] J. Cho, F. Caruso, Chem. Mater. 17 (2005) 4547.
[5] G. Decher, Science 277 (1997) 1232.
[6] G. Decher, Y. Lvov, J. Schmitt, Thin Solid Films 244 (1994) 772.
[7] C.F.J. Faul, M. Antonietti, Adv. Mater. 15 (2003) 673.
[8] K. Ariga, Y. Lvov, T. Kunitake, J. Am. Chem. Soc. 119 (1997) 2224.
[9] J. Lang, M.H. Lin, J. Phys. Chem. B 103 (1999) 11393.
[10] S.L. Clark, E.S. Handy, M.F. Rubner, P.T. Hammond, Adv. Mater. 11 (1999) 1031.
[11] D.J. Zhou, A. Bruckbauer, L.M. Ying, C. Abell, D. Klenerman, Nano Lett. 3 (2003) 1517.

[12] C.A. Constantine, S.V. Mello, A. Dupont, X.H. Cao, D. Santos, O.N. Oliveira, F.T. Strixino, E.C. Pereira, T.C. Cheng, J.J. Defrank, R.M. Leblanc, J. Am. Chem. Soc. 125 (2003) 1805.
[13] N.A. Kotov, I. Dékány, J.H. Fendler, J. Phys. Chem. 99 (1995) 13065.
[14] A.D. Pris, M.D. Porter, Nano Lett. 2 (2002) 1087.
[15] C.L. Hill (Ed.), Chem. Rev. 98 (1998) 1.
[16] N. Fay, E. Dempsey, T. McCrmac, J. Electroanal. Chem. 574 (2005) 359.
[17] S.O. Liu, D.G. Kurth, H. Möhwald, D. Volkmer, Adv. Mater. 14 (2002) 225.
[18] L. Cheng, J. Liu, S. Dong, Anal. Chim. Acta 417 (2000) 133.
[19] G. Gao, L. Xu, W. Wang, W. An, Y. Qiu, Z. Wang, E. Wang, J. Phys. Chem. B 109 (2005) 8948.
[20] L. Xu, H. Zhang, E. Wang, D.G. Kurth, Z. Li, J. Mater. Chem. 12 (2002) 654.
[21] A. Kuhn, F.C. Anson, Langmuir 12 (1996) 5481.
[22] G.M. Kloster, F.C. Anson, Electrochim. Acta 44 (1999) 2271.
[23] H. Ma, J. Peng, Y. Chen, Y. Feng, E. Wang, J. Solid State Chem. 177 (2004) 3333.
[24] C.A. Goss, H.D. AbruŃa, Inorg. Chem. 24 (1985) 4263.
[25] F. Tobalina, F. Pariente, L. Hernández, H.D. AbruŃa, E. Lorenzo, Anal. Chim. Acta 395 (1999) 17.
[26] C. Rocchiccioli-Deltcheff, M. Fournier, R. Franck, R. Thouvenot, Inorg. Chem. 22 (1983) 207.
[27] R.G. Finke, M.W. Droege, P.J. Domaille, Inorg. Chem. 26 (1987) 3886.
[28] W. Paw, R. Eisenberg, Inorg. Chem. 36 (1997) 2287.
[29] L. Ruhlmann, L. Nadjo, J. Canny, R. Contant, R. Thouvenot, Eur. J. Inorg. Chem. 4 (2002) 975.
[30] S. Liu, Z. Tang, Z. Wang, Z. Peng, E. Wang, S. Dong, J. Mater. Chem. 10 (2000) 2727.
[31] W. Sun, F. Yang, H. Liu, J. Kong, S. Jin, G. Xie, J. Deng, J. Electroanal. Chem. 451 (1998) 49.
[32] L. Ruhlmann, G. Genet, J. Electroanal. Chem. 568 (2004) 315.
[33] J.N. Younathan, K.S. Rhodes, T.J. Meyer, Inorg. Chem. 31 (1992) 3280.
[34] D. Martel, A. Kuhn, Electrochim. Acta 45 (2000) 1829.
[35] F. Matsumoto, S. Uesugi, N. Koura, T. Ohsaka, J. Electroanal. Chem. 549 (2003) 71.